Acta Scientiarum

http://www.uem.br/acta
ISSN printed: 1806-2563
ISSN on-line: 1807-8664
Doi: 10.4025/actascitechnol.v35i3.15554

Numerical investigation of flow induced by a disc turbine in unbaffled stirred tank

Houari Ameur* **and Mohamed Bouzit**

*Faculté de Génie Mécanique, Université des Sciences et Technologies Mohamed Boudiaf, B.P. 1505, El M'nouar, Oran, Algérie. *Author for correspondence. E-mail: houari_ameur@yahoo.fr*

ABSTRACT. The flow generated by a disc turbine in a cylindrical unbaffled tank was numerically modeled. This study was carried out for shear-thinning fluids. Analyses concern the effect of impeller rotational speed, fluid rheology and impeller blade curvature on the mean velocities and power consumption. It was found that the cavern size and the power consumption are higher for extreme shear thinning fluids. It was found also that the best performance is achieved at high Reynolds number and flat-blade turbine. Predictions have been compared with literature data and a satisfactory agreement has been found.

Keywords: numerical study, stirred tank, shear thinning fluid, disc turbine, impeller location, blade curvature.

Investigação numérica do fluxo induzido por uma turbina de disco em 'unbaffled' tanque de agitação

RESUMO. O fluxo gerado por uma turbina de disco em um tanque cilíndrico unbaffled foi numericamente modelada. Este estudo foi realizado para corte fino fluidos. As análises dizem respeito ao efeito da velocidade de rotação do rotor, reologia de fluidos e curvatura da lâmina do rotor na velocidade média e consumo de energia. Verificou-se que o tamanho da caverna eo consumo de energia são maiores para diluir os fluidos de corte extremas. Verificou-se também que o melhor desempenho é alcançado em número de Reynolds alto e flat-blade turbina. Previsões foram comparados com dados da literatura e um acordo satisfatório foi encontrado.

Palavras-chave: estudo numérico, tanque de agitação, fluido pseudoplástico, disco turbina, localização do rotor, a curvatura da lâmina.

Introduction

Mixing operations with non-Newtonian fluids are frequently employed in areas such as the food, pharmaceutical, paint, or polymer industries. Additional difficulties for the optimization of processes often occur with such fluids. In fact, the hydrodynamics strongly depends on the nature of the fluids involved in the mixing system.

Shear thinning fluids are an important class of non-Newtonian fluids. Mixing of these fluids in mechanically stirred tanks has been found to cause the formation of a zone of intense motion around the impeller (the so called cavern) with essentially stagnant regions elsewhere (MOORE et al., 1995; WILKENS et al., 2005). The formation of a cavern in these stirred tanks resulted in diminished mixing of the fluid in the tank, and is thus undesirable. The formation of such a cavern in a mechanical stirred vessel has been found to form in certain slurries and operating conditions (BAKKER et al., 2009), effectively reducing the active volume of the vessel where mixing occurs, since a high rate of turbulent energy dissipation, required for the flotation of fine particles (DEGLON, 2005; SCHUBERT, 2008), would be absent in the stagnant regions of slurry.

Since non-Newtonian fluids encountered in industry are often solid suspensions and therefore opaque, many experimental techniques traditionally used to measure local fluid flow are unsuitable. In an attempt to be able to predict the shape and size of the cavern formed in these fluids, various researchers have developed empirical and mathematical models to calculate the cavern dimensions (AMANULLAH et al., 1998; SOLOMON et al., 1981; WILKENS et al., 2005).

Pakzad et al. (2007) have investigated the flow pattern generated by a Scaba impeller for mixing yield stress fluid. Pakzad et al. (2008) have used the electrical resistance tomography (ERT) technique to examine, in three dimensions, the homogeneity and flow pattern inside the mixing tank. They have studied the shape and the size of cavern generated around a radial-flow Scaba 6SRGT impeller in the

mixing of xanthan gum solution, which is a pseudoplastic fluid possessing yield stress.

By using ultrasonic Doppler velocimetry and CFD modeling, Ein-Mozaffari and Upreti (2009) have investigated the mixing of yield stress fluids by a radial impeller. Bakker et al. (2010) have developed a semi-empirical model to calculate the height of caverns forming in non-Newtonian mineral slurries in a mechanical flotation cell. Guida et al. (2010) have used particle image velocimetry (PIV) to determine the complex flow field in mechanically agitated vessels with a pitched blade turbine, the fluid used here is Newtonian. Vishalkumar et al. (2011) have developed three dynamic models to characterize the continuous mixing of xanthan gum solutions.

Thorough search of the literature suggests that no space has been devoted to the study of agitation of power law fluids by curved bladed impeller. Therefore, the objective of the present paper is to employ advanced computational fluid dynamics (CFD) to study the flow patterns and power consumption for stirring power law fluids with a disc turbine. Our attention is focused on the effects of impeller rotational speed, fluid rheology and impeller blade curvature. The study is restricted to the laminar and transition regimes with shear thinning fluids, which are typical conditions of polymerization reactions.

Material and methods

Flow equations

We assume that the flow is fully periodic, making it possible to use a Lagrangian viewpoint to simulate a steady three-dimensional flow in the mixer. In this rotating frame of reference, the impeller remains fixed and the vessel rotates in the opposite direction (the observer is moving with the impeller). The corresponding flow equations are:

$$\rho\left(V\,grad\,V+\omega(\omega R)+2\omega V\right)+grad\,p-div\left(2\eta\left(\dot{\gamma}\right)\dot{\gamma}\right)=0 \quad (1)$$

$$div\,V=0 \quad (2)$$

In equation (1), $\dot{\gamma}=\left(\frac{1}{2}\right)\left[grad\,V+(grad\,V)^{T}\right]$ is the rate-of-strain tensor, $\omega(\omega R)$ the centrifugal acceleration, $2\omega V$ the Coriolis acceleration, R the radial coordinate and $\omega=(\omega_x,\omega_y,\omega_z)$ the angular velocity in clockwise direction. The boundary conditions are:

- At the vessel wall and bottom: $V=\omega R$
- On the impeller: $V=0$

A series of shear thinning fluids obeying the power-law model are considered: the consistency index is 8 Pa s^n, and the power law indices range from 0.4 to 1. In all the computations, the fluid density is 1394 kg m^{-3}. The above equations are solved using the finite volume method.

For a shear thinning fluid (Ostwald model), the Reynolds number is given by:

$$Re_g=\frac{\rho N^{2-n}D^2}{m} \quad (3)$$

Mixer configurations

The mixing configuration consists of a cylindrical unbaffled tank with a flat bottom (Figure 1), the liquid level H is equal to the diameter vessel D, with D = 300 mm. The impeller contains four blades fixed on a disc with 20 mm of diameter and 3 mm of thickness, which is attached on a cylindrical central shaft of diameter d/D = 0.05. The effect of the curvature blade has been investigated, for this task, four impellers were used: flat-blade with a height of 20 mm, and three curved-blades, which have a curvature radius $r^\star = r/D$ = 0.02, 0.042 and 0.064, respectively (Figure 2). We note that all of these impellers have the same blade perimeter h = 20 mm, the same diameter d/D = 0.5 and placed at the same clearance from the tank bottom: c/D = 0.5.

All variables describing the hydrodynamic state are writing in dimensionless form, the dimensionless forms of velocities, radial (R) and axial (Z) coordinates are obtained as follow: $V^\star = V/\pi ND$; $R^\star = 2R/D$ and $Z^\star = Z/D$.

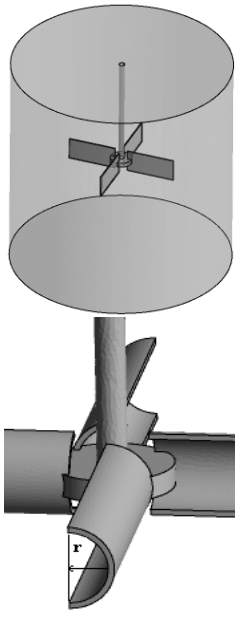

Figure 1. Mixing system.

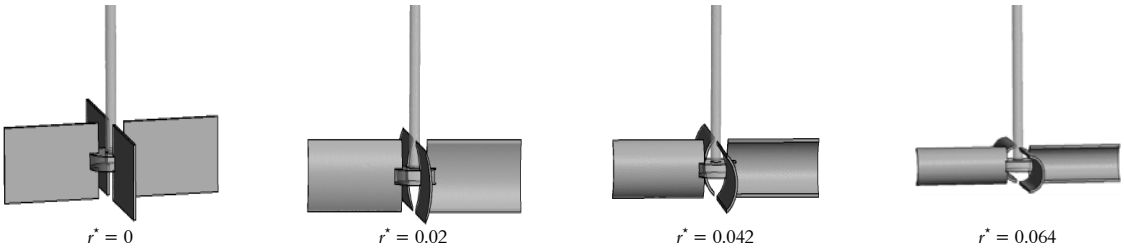

Figure 2. Impellers used in the study.

Numerical details

The 3D flow field generated by a disc turbine in the agitation of shear thinning fluid was simulated using the commercial CFD package (CFX 12.0).

In the present paper, constant boundary conditions have been set respecting a rotating reference frame (RRF) approach. Here, the impeller is kept stationary and the flow is steady relative to the rotating frame, while the outer wall of the vessel is given an angular velocity equal and opposite to the velocity of the rotating frame. This approach can be employed due to the absence of baffles.

A pre-processor (ICEM CFD 12.0) was used to discretize the flow domain with a tetrahedral mesh. In general, the density of cells in a computational grid needs to be fine enough to capture the flow details, but not so fine, since problems described by large numbers of cells require more time to solve. In order to capture the boundary layer flow detail, an increased mesh density was used near the tank wall and the rotating impeller. In order to have a very refined mesh in the vicinity of the blades, the sufficient amount of nodes that properly define the curvature of the blades was created on the impeller edges and a size function was used to control the mesh growth. This feature allows the mesh elements to grow slowly as a function of the distance from the impeller blades. The number of cells used for discretization was determined by conducting a grid independence study.

Mesh tests were performed by verifying that additional cells did not change the velocity magnitude in the regions of high velocity gradients around the impeller blades by more than 2.5%.

Simulations were considered converged when the scaled residuals for each transport equation were below 10^{-7}. Most simulations required about 2000 iterations for convergence. This study is restricted to the laminar and transition regimes, the Reynolds number is varying from 0.1 to 160. The transition regime begins for Reynolds number between 20 and 30 for this kind of fluids (Figure 5). Even if the flow is not fully into the turbulent regime, we should simulate the flow as being turbulent. Fortunately, the turbulent properties vanish when in the laminar flow, so the correct way of simulating in the transitional regime is using a turbulence model. In our study, we have used the SST model. This model has the option of specifying how we model the transition turbulence: it is the fully turbulent, specified intermittency (requiring acquired knowledge), the gamma model or the gamma theta model.

Results and discussion

This section presents the numerical results obtained for a shear thinning fluid flow in the whole volume stirred. Firstly, it seems necessary to validate the CFD computer code; for this task, we have reffered to the review of Mishra et al. (1998) and we have realized the same geometrical parameters.

We note that Mishra et al. (1998) used laser Doppler anemometry to measure the flow generated by a disc turbine in aqueous solutions of polyacrylamide (PAA) (molecular weight: $5 \times 10^6 - 6 \times 10^6$) in a cylindrical tank. The tank diameter was 300 mm, with a flat bottom. The disc turbine was 100 mm in diameter and was centrally located. The liquid height was kept equal to the vessel diameter.

At a radial position $R = R_i + 3$ mm (R_i : impeller radius) and for the water, predicted results for radial velocity ($V_r^\star$) along the vessel height ($Z^\star = Z/D$) were releaved and presented on Figure 3. The Comparison between our results and those given by Mishra shows a good agreement.

In this paper, we have investigated the effect of impeller blade curvature. For this purpose and in order to check again the validity of the CFD model and the numerical method used, we have referred to a work using an impeller with curved blade (PAKZAD et al., 2007). We note here that similar geometrical conditions as those chosen by Pakzad were considered; also the same fluid is simulated. Predicted results for power number are presented on Figure 4 and compared with those of Pakzad et al. (2007): a satisfactory agreement is observed.

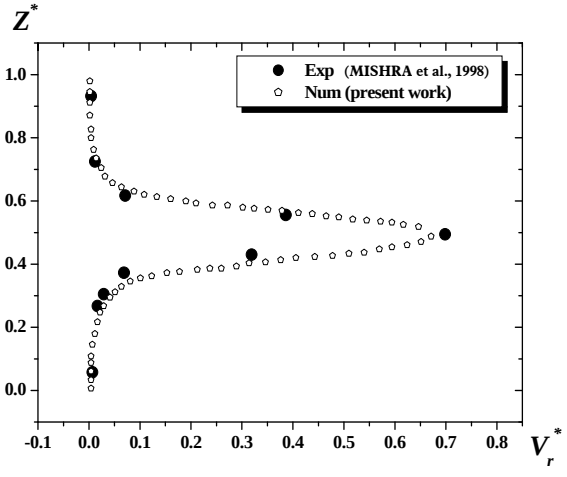

Figure 3. Axial profile of mean radial velocity.

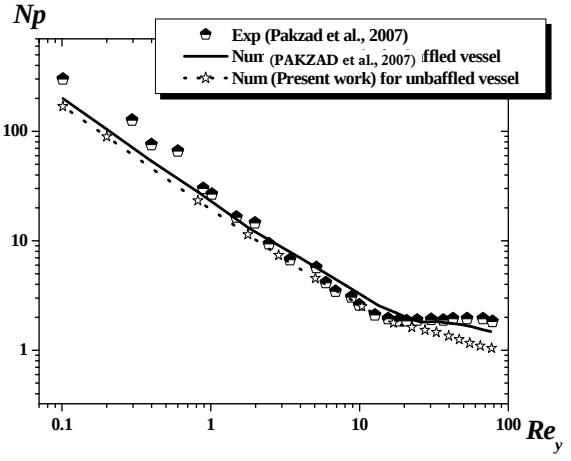

Figure 4. Power number for $n = 0.12$, $d/D = 0.315$, $c/D = 0.425$, $h/D = 0.12$.

Effect of impeller rotational speed

We begin the analysis by testing the effect of impeller rotational speed on the flow fields generated. The study is restricted to the laminar and transition regimes, in a range of Reynolds number varying from 0.1 to 160. The origin of the tangential coordinate is located on a paddle.

This type of impeller generates a radial flow, a stream impinging from the blade is directed horizontally to the vessel wall and divided into two flows: one downward to the tank bottom and redirected vertically to the impeller, the other upward to the free surface of liquid and going along the impeller shaft forming then two recirculation loops. For details on the vortex size generated by this type of turbine, we have presented in Figure 5 the axial velocity component along the vessel height. The minus sign of V_z^* indicates the existing of recirculation flow. For the first case: $Re_g = 10$, no recirculation is marked, but for the other cases, the vortices are present and increase continuously with Re_g.

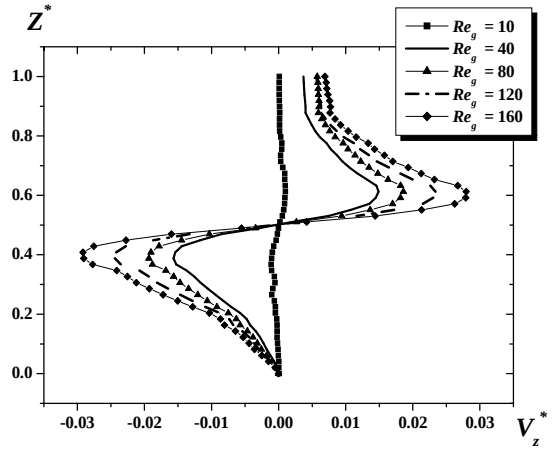

Figure 5. Axial velocity for $n = 0.7$, $R\star = 0.7$, $r^* = 0$.

The agitation of pseudoplastic fluids results in the formation of a well mixed region (cavern) around the impeller and essentially stagnant and/or slow moving fluids elsewhere in the vessel.

Figure 6 illustrates the velocity contours obtained for a power law index $n = 0.7$. If the Reynolds number is lower, the zone of intense motion is limited in the area swept by the turbine, but the increase of this parameter (Re_g) yields a wider cavern.

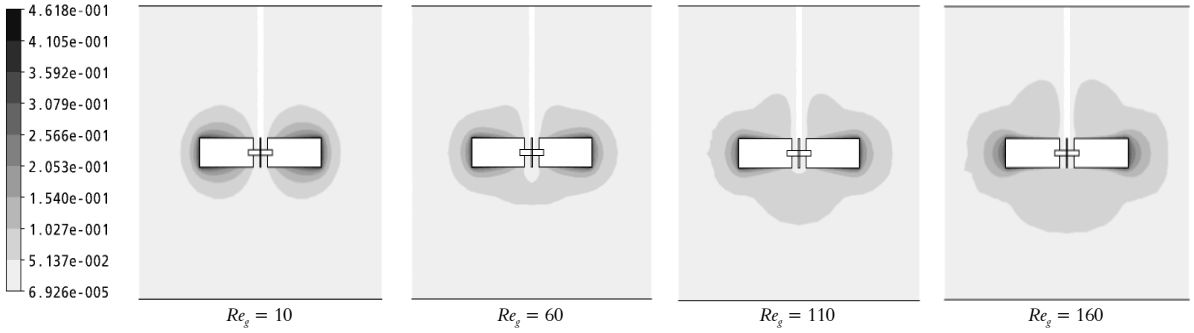

Figure 6. Velocity contours induced at $n = 0.7$, $r^* = 0$.

Effect of fluid rheology

The rheological parameters of the fluid have also an important effect on the flow fields generated. For this task, four values of the structural index (n) were chosen (0.4, 0.6, 0.8 and 1). In Figure 7, the tangential velocity profiles as a function of the vessel radius, at the mid-height of the impeller blade, show a maximum at the blade tip for any value of the structural index, but if this parameter (n) is more lower, the momentum transfer is less intense, because of the viscous forces, which explains the speed decay curves (for n = 0.8, 0.6 and 0.4, respectively).

For more illustrations about the effect of the rheological behavior on the hydrodynamic induced, we have presented on Figure 8 the velocity contours. As it is shown, the increase in power law index produces larger recirculation loop and wider well mixing region.

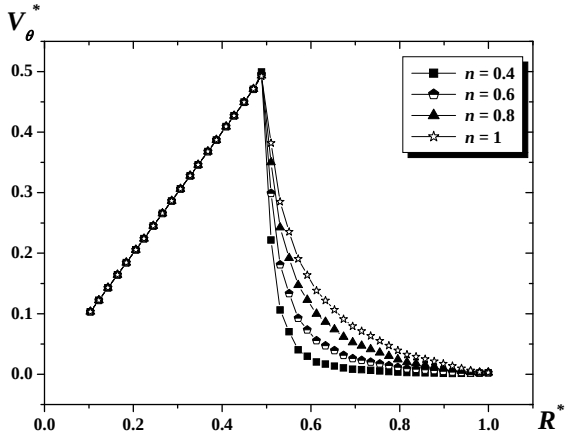

Figure 7. Tangential velocity for Re_g = 20, Z^* = 0.5, r^* = 0.

The mixing power constitutes a global parameter to describe the performances of a mechanically stirred system, it is a macroscopic result obtained by integration on the impeller surface of the local power transmitted by the impeller to the fluid. It is quite equivalent to say that the power consumption P is entirely given by the impeller to the fluid. In these conditions:

$$P=\eta \int_{vessel\ volume} Q_v\, dv \tag{4}$$

The dimensional analysis enables us to characterize power consumption through the power number N_P which is calculated as:

$$N_P=\frac{P}{\rho N^3 D^5} \tag{5}$$

Figure 9 presents the variations of N_P versus of Re_g in a logarithmic scale, it can be seen that at Reynolds number less than 10 the power number changes linearly with the slope of -1.

In the transition regime, this variable changes slightly with Re_g. On the other hand, for a flow index more pronounced the power provided is more important.

Effect of the curvature blade

Various types of impellers are used in mechanically agitated vessels in order to fulfill different mixing requirements in industry. Conventional impeller types such as standard Rushton impellers, pitched-blade impellers and various propellers are still widely used in practice because of their relatively well established design methods. In the last two decades, a number of new, modified impellers have been developed to improve the performance of conventional impellers. Typical examples are concave-blade impellers.

Van't Riet et al. (1976) studied a variety of impeller styles, and introduced the concept of using concave blades. Warmoeskerken and Smith (1989) extended that work and explained the improved performance of the concave blades compared to flat blades in terms of reduced cavity formation behind the blades. Impellers with a semicircular blade shape are now common in the industry, e.g. the Chemineer CD-6 (BAKKER et al., 1994) and the Scaba 6SRGT impeller (PAKZAD et al., 2008).

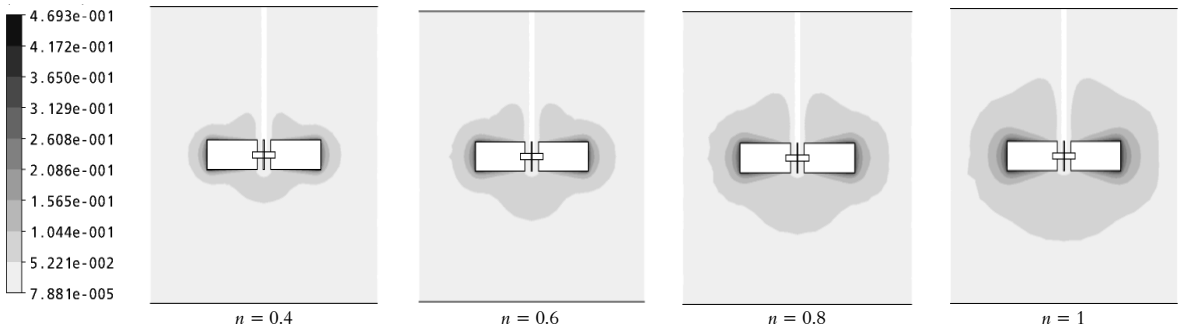

Figure 8. Velocity contours for Re_g = 100, r^* = 0.

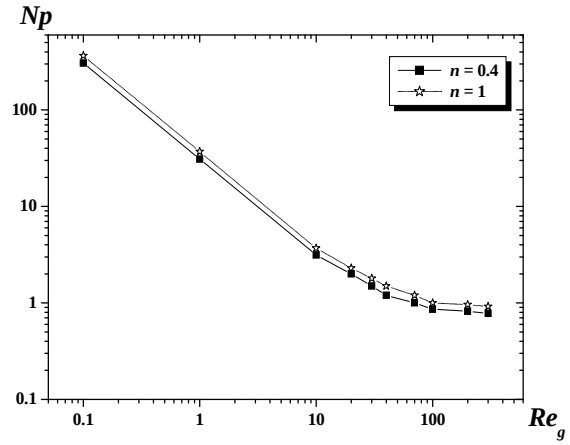

Figure 9. Power number for $r^* = 0$.

Warmoeskerken and Smith (1989) reported that the gas-liquid mass transfer in an agitated tank due to a semi-circular blade impeller is at least 20% higher than that of a standard Rushton impeller at high power dissipation levels. It should be noted that experiments by Linek et al. (1991) showed a decrease in k_{La} by a simple change from Rushton turbines to semi-circular blade impellers.

Chen and Chen (1999) found that, at the high k_{La} level, the mass transfer coefficients obtained using the concave-blade impellers are slightly higher than those using the Rushton impeller under the same gassed power level and aeration rate. It is known that the dimension of the cavity behind an impeller blade increases with an increase in the impeller speed and a smaller cavity was found to form behind a concave blade (WARMOESKERKEN; SMITH, 1989). It has also been shown by Mishra and Joshi (1993) that the pumping capacity of a semi-circular blade impeller is much higher than that of a Rushton impeller. The cavity size and the pumping capacity are believed to change gradually with an increase in the blade curvature at least up to $e = 0.5$. Further increase in the blade curvature may results in a smaller cavity size, but may decrease the pumping capacity as well due to the blockage of fluid flow by the curved blade.

Cooke end Heggs (2005) found that, when compared at conditions above the minimum Froude number required to disperse gas, the hollow blade turbines (HBT) designs are as energetically efficient as Rushton turbines for dispersing gas.

Chemineer (2011) claim on their website that the CD-6 can handle about 2.4 times the maximum gas capacity of the D-6 (Rushton turbine) impeller and that the DT-6 can disperse nearly six times the gas handling capability of the D-6.

Cooke and Heggs (2005) found that, for the suspension of high levels of solids the $d = D/2$ hollow blade turbines, at a clearance of $D/4$, are the most efficient agitators especially under gassed conditions, where almost no effect of gassing on the just suspension speeds were noted.

The impeller design is an important parameter for enhancing quality, capacity, process efficiency and energy efficiency of a mixing system. For meeting these objectives, it is imperative that the relationship between the flow pattern and the design objective is understood. One of the flow characteristics affecting the impeller flow efficiency is the presence of trailing vortices generated at the tip of the impeller blades.

In this section, the effect of the curvature blade is investigated. We based on the characteristics of flow field and power consumption for stirring shear thinning fluids. For this purpose, four geometrical configurations are realized: $r^* = 0$ which is corresponding to the flat blade, and three other impellers with curved blades: $r^* = 0.02$, $r^* = 0.042$ and $r^* = 0.064$.

From the computation results presented in this section, we can remark that:

The flow is radial for any case, and there are two recirculation loops generated in the vessel volume (Figures 10), but these eddies reduce in size with the increase in curvature blade: the flat-blade produces the higher radial stream than the other cases. With the flat-blade turbine, the liquid surface swept is the largest, which gives wider cavern (Figure 11), but the required mixing power is more pronounced (with the decrease of r^*) (Figure 12).

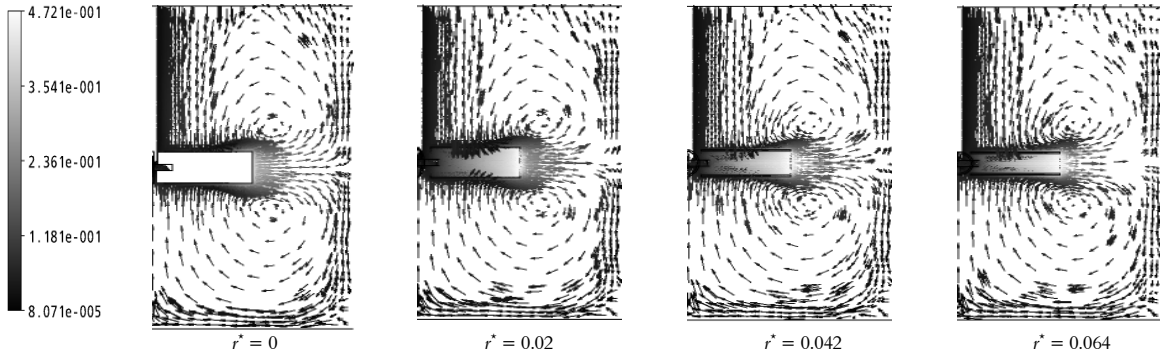

Figure 10. Velocity vectors for $Re_g = 160$, $n = 0.9$.

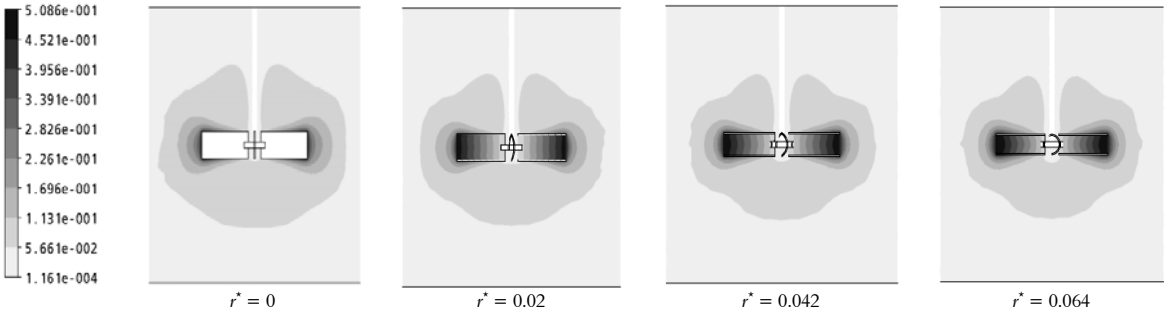

Figure 11. Velocity contours induced at $Re_g = 100$, $n = 0.9$.

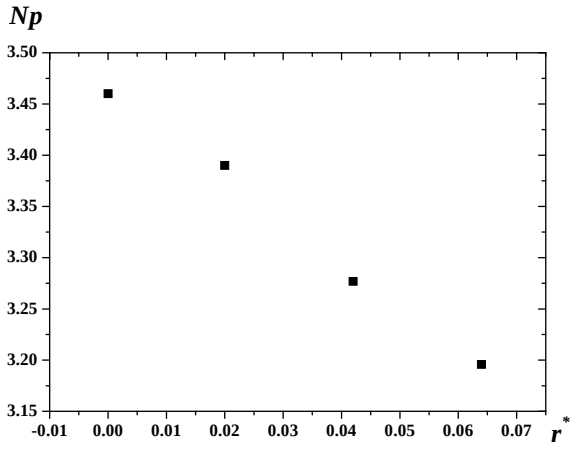

Figure 12. Power number for $n = 0.7$, $Re_g = 10$.

From these results and based on the finding of the above references, in order to reduce the mixing power, it is recommended to use a curved bladed impeller. But the excessive increase in the blade curvature can reduce the cavern size. Therefore a very deep hollow bladed is not required, due to the blockage of fluid flow by the curved blade.

Conclusion

The objective of this paper was to investigate the flow and mixing in a vessel equipped with a disc turbine. The flow fields and the mixing structures were computed for Reynolds number ranging in the laminar and transitions regimes. The effect of the Reynolds number, the fluid rheology and the impeller blade curvature on its performance has been studied. The cavern size and the power consumption are higher for extreme shear thinning fluids. The Reynolds number and the impeller blade curvature also strongly influence the cavern size and the mixing power. The best performance is achieved at Reynolds number upper to 20 and curved bladed turbine, not with a very deep curvature, because the further increase in the blade curvature may results in a smaller cavern size, and may decreases the pumping capacity as well due to the blockage of fluid flow by the curved blade.

References

AMANULLAH, A.; HJORTH, S. A.; NIENOW, A. W. A new mathematical model to predict cavern diameters in highly shear thinning, power law liquids using axial flow impellers. **Chemical Engineering Science**, v. 53, n. 3, p. 455-469, 1998.

BAKKER, A.; MYERS, K. J.; SMITH, J. M. How to disperse gases in liquids. **Chemical Engeenering**, v. 101, n. 12, p. 98-104, 1994.

BAKKER, C. W.; MEYER, C. J.; DEGLON, D. A. Numerical modeling of non-Newtonian slurry in a mechanical flotation cell. **Minerals Engineering**, v. 22, n. 11, p. 944-950, 2009.

BAKKER, C. W.; MEYER, C. J.; DEGLON, D. A. The development of a cavern model for mechanical flotation cells. **Minerals Engineering**, v. 23, n. 11-13, p. 968-972, 2010.

CHEMINEER. **Reability and technology in mixing**. Available from: <http://www.chemineer.com>. Access on: Nov. 20, 2011.

CHEN, Z. D.; CHEN, J. J. J. Comparison of mass transfer performance for various single and twin impellers. **Chemical Engineering Research and Design**, v. 77, n. 2, p. 104-109, 1999.

COOKE, M.; HEGGS, P. J. Advantages of the hollow (concave) turbine for multi-phase agitation under intense operating conditions. **Chemical Engineering Science**, v. 60, n. 20, p. 5529-5543, 2005.

DEGLON, D. A. The effect of agitation on platinum ores. **Minerals Engineering**, v. 18, n. 8, p. 839-844, 2005.

EIN-MOZAFFARI, F.; UPRETI, S. R. Using ultrasonic Doppler velocimetry and CFD modeling to investigate the mixing of non-Newtonian fluids possessing yield stress. **Chemical Engineering Research and Design**, v. 87, n. 4, p. 515-523, 2009.

GUIDA, A.; NIENOW, A. W.; BARIGOU, M. The effects of the azimuthal position of the measurement plane on the flow parameters determined by PIV within a stirred vessel. **Chemical Engineering Science**, v. 65, n. 8, p. 2454-2463, 2010.

LINEK, V.; BENES, P.; SINKULE, J. The hollow blade agitator for mass transfer in gas-liquid bioreactors, **Trans IChemE, Food and Bioproducts Processing**, v. 69, n. C3, p. 145-148, 1991.

MISHRA, V. P.; JOSHI, J. B. Flow generated by a disc turbine: part III: effect of impeller diameter, impeller

location and comparison with other radial flow turbines. **Trans IChemE, Chemical Engineering Research and Design**, v. 71, n. 5, p. 563-573, 1993.

MISHRA, V. P.; KUMAR, P.; JOSHI, J. B. Flow generated by a disc turbine in aqueous solutions of polyacrylamide. **Chemical Engineering Journal**, v. 71, n. 1, p. 11-21, 1998.

MOORE, I. P. T.; COSSOR, G.; BAKER, M. R. Velocity distributions in a stirred tank containing a yield stress fluid. **Chemical Engineering Science**, v. 50, n. 15, p. 2467-2481, 1995.

PAKZAD, L.; EIN-MOZAFFARI, F.; CHAN, P. Using computational fluid dynamics modelling to study the mixing of pseudoplastic fluids with a Scaba 6SRGT impeller. **Chemical Engineering and Processing**, v. 47, n. 12, p. 2218-2227, 2007.

PAKZAD, L.; EIN-MOZAFFARI, F.; CHAN, P. Using electrical resistance tomography and computational fluid dynamics modeling to study the formation of cavern in the mixing of pseudoplastic fluids possessing yield stress. **Chemical Engineering Science**, v. 63, n. 9, p. 2508-2522, 2008.

SCHUBERT, H. On the optimization of hydrodynamics in fine particle flotation. **Minerals Engineering**, v. 21, n. 12-14, p. 930-936, 2008.

SOLOMON, J.; ELSON, T. P.; NIENOW, A. W.; PACE, G. W. Cavern sizes in agitated fluids with a yield stress. **Chemical Engineering Communications**, v. 11, n. 1-3, p. 143-164, 1981.

VAN'T RIET, K.; BOOM, J. M.; SMITH, J. M. Power consumption, impeller coalescence and recirculation in aerated vessels. **Trans IChemE**, v. 54, n. 1, p. 124-131, 1976.

VISHALKUMAR, R. P.; EIN-MOZAFFARI, F.; UPRETI, S. R. Effect of time delays in characterizing the continuous mixing of non-Newtonian fluids in stirred tank reactors. **Chemical Engineering Research and Design**, v. 89, n. 10, p. 1919-1928, 2011.

WARMOESKERKEN, M. M. C. G.; SMITH, J. M. The hollow blade agitator for dispersion and mass transfer. **Trans IChemE, Chemical Engineering Research and Design**, v. 67, n. 2, v. 193-198, 1989.

WILKENS, R. J.; MILLER, J. D.; PLUMMER, J. R.; DIETZ, D. C.; MEYERS, K. J. New techniques for measuring and modeling cavern dimensions in a Bingham plastic fluid. **Chemical Engineering Science**, v. 60, n. 19, p. 5269-5275, 2005.

Received on December 19, 2011.
Accepted on March 5, 2012.